Available online at www.sciencedirect.com
ScienceDirect
Journal of Computational and Applied Mathematics 218 (2008) 247–258
JOURNAL OF COMPUTATIONAL AND APPLIED MATHEMATICS
www.elsevier.com/locate/cam

Stable cycles in a Cournot duopoly model of Kopel

W. Govaerts[a,*], R. Khoshsiar Ghaziani[a,b]

[a] Department of Applied Mathematics and Computer Science, Ghent University, Krijgslaan 281-S9, B-9000 Gent, Belgium
[b] Department of Mathematics, Faculty of Science, Shahrekord University, PO Box 115, Shahrekord, Iran

Received 17 August 2006; received in revised form 13 November 2006

Abstract

We consider a discrete map proposed by M. Kopel that models a nonlinear Cournot duopoly consisting of a market structure between the two opposite cases of monopoly and competition. The stability of the fixed points of the discrete dynamical system is analyzed. Synchronization of two dynamics parameters of the Cournot duopoly is considered in the computation of stability boundaries formed by parts of codim-1 bifurcation curves. We discover more on the dynamics of the map by computing numerically the critical normal form coefficients of all codim-1 and codim-2 bifurcation points and computing the associated two-parameter codim-1 curves rooted in some codim-2 points. It enables us to compute the stability domains of the low-order iterates of the map. We concentrate in particular on the second, third and fourth iterates and their relation to the period doubling, 1:3 and 1:4 resonant Neimark–Sacker points.

MSC: 39A10

Keywords: Bifurcation of fixed points; Cycles; Normal form coefficients; Bistability

1. Introduction

The first well-known model which gives a mathematical description of competition in a duopoly market dates back to the French economist Cournot [13] with the highlighted characteristics:

- Competing firms produce goods that are perfect substitutes.
- Both firms must consider the actions and reactions of the competitor.
- Each firm forms expectations of the other firm's output in order to determine a profit maximizing quantity to produce in the next time period (this situation is called strategic interdependence).

The model that he presented has been much studied for its ability to generate complex dynamics and also because of its more general foreshadowing of game theory. It has often been noted that the Cournot equilibrium is but a special case of the Nash Equilibrium [21], the more general formulation used by modern industrial organization economists in studying oligopoly theory.

* Corresponding author.
E-mail address: Willy.Govaerts@UGent.be (W. Govaerts).

0377-0427/$ - see front matter © 2007 Elsevier B.V. All rights reserved.
doi:10.1016/j.cam.2007.01.012

Recently, several works have shown that the Cournot model may lead to complex behaviors such as cyclic and chaotic, see, for example [1,17,22–24]. Among the first to do this was Puu [22,23] who found a variety of complex dynamics arising in the Cournot duopoly case including the appearance of attractors with fractal dimension. Dynamics of a Cournot game by players with bounded rationality has been studied in [5]. Local stability of a duopoly game with heterogeneous expectation has been studied in [4]. Multistability, cyclic and chaotic behavior of a Cournot game have been studied in [9], where in the model the reaction functions have the form of the logistic map. Some preliminary results on the local bifurcations of a Kopel map were obtained in [17]. Explicit boundaries of local stability of the fixed point of a Kopel map have been derived in [2]. Basins of attraction in a Kopel map have been studied in [8]. Other studies on the dynamics of oligopoly models with more firms and other modifications include Ahmed and Agiza [6], Agiza [1] and Agiza et al. [3]. The development of complex oligopoly dynamics theory has been reviewed in [25].

In this paper we consider the general case of a duopoly model, see [2], introduced in [17] with positive adjustment coefficient ρ. The main aim is to investigate the overall dynamic behavior of the model when $\rho > 0$ and to compute stability domains of the first, second, third and fourth iterates of the map. In Section 2 we introduce the model and discuss the general stability and branching of the fixed points. In particular, we compute analytically the critical normal form coefficients in the case of period doubling bifurcations to reveal sub- or supercriticality. In Section 3 we concentrate on the economically relevant case $\rho \leqslant 1$ and numerically compute curves of codim-1 bifurcations and the critical normal form coefficients of codim-2 bifurcation points, using the new software CL_MATCONTM [14,16]. These tools enable us to compute stability boundaries of 2, 3 and 4-cycles. Furthermore, by considering the critical normal form coefficients of the $R4$ resonance point, we determine the bifurcation scenario of the map near this point.

In Section 4 we briefly describe $R3$ and $R2$ bifurcation points in the region $\rho > 1$ which is of no interest for the economic model. In Section 5 we summarize our results and draw some conclusions.

2. The map and the local stability analysis of its fixed points

The model that we use is a two-dimensional map described in [17,2]. Two firms are homogeneous with regard to their expectation formation and the action effect on each other. The duopoly Kopel model assumes that at each discrete time t the two firms produce the quantities $x_1(t)$ and $x_2(t)$, respectively, and decide their productions for the next period $x_1(t+1)$ and $x_2(t+1)$. The time evolution of the model is determined by the two-dimensional map $T : (x_1(t), x_2(t)) \rightarrow (x_1(t+1), x_2(t+1))$ defined by

$$T : \begin{cases} x_1(t+1) = (1-\rho)x_1(t) + \rho\mu x_2(t)(1 - x_2(t)), \\ x_2(t+1) = (1-\rho)x_2(t) + \rho\mu x_1(t)(1 - x_1(t)), \end{cases} \tag{1}$$

where ρ and μ are two model parameters. The positive parameter μ measures the intensity of the effect that one firm's actions has on the other firm. Firms do not change their productions according to the computed optimal productions (i.e., the 'logistic' reaction functions) but they prefer to choose a weighted average between the previous production and the computed one, with weights $1-\rho$ and ρ, respectively; ρ is called the adjustment coefficient. The meaning of the model implies that the parameter $\rho \in [0, 1]$. However, it is best to ignore this restriction in a first global study of the properties of the model, cf. [2].

2.1. Fixed points of the map

Bifurcation of maps have been studied intensively in the literature, cf [20,12,11,10]. A comprehensive discussion is given in [18]. We further use the recent results in [16,19].

The fixed points of (1) and their stability were studied analytically in [2, Section 2.1–4]. We summarize the obtained results briefly. For $\rho \neq 0$, the fixed points of (1) are the solutions to

$$x_1^* = \mu x_2^*(1 - x_2^*), \quad x_2^* = \mu x_1^*(1 - x_1^*). \tag{2}$$

Besides the trivial solution $E_1 : (x_1^*, x_2^*) = (0, 0)$, a positive symmetric fixed point exists for $\mu > 1$, given by $E_2 : (x_1^*, x_2^*) = ((\mu - 1)/\mu, (\mu - 1)/\mu)$.

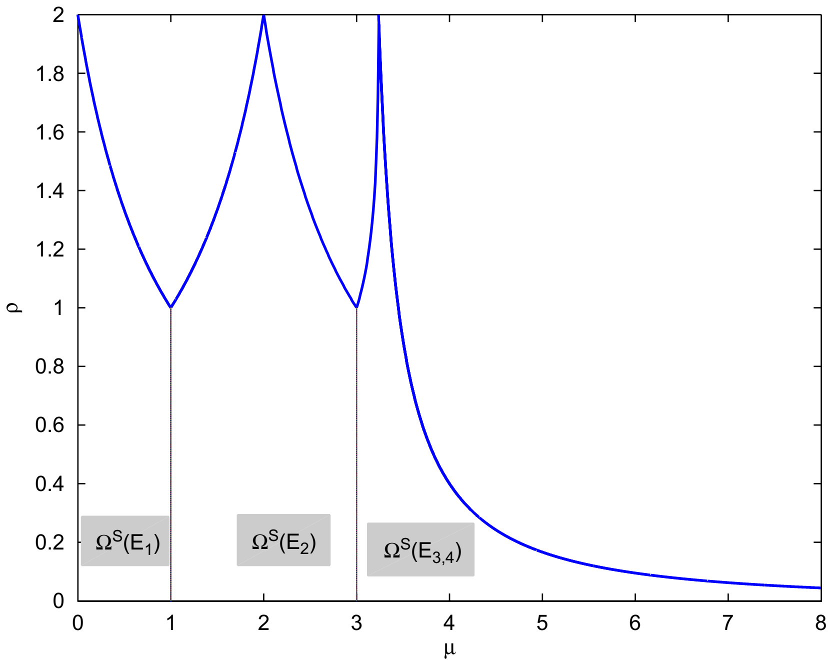

Fig. 1. Stable regions of E_i, $i = 1, 2, 3, 4$.

Two further nonsymmetric Nash Equilibria, given by

$$E_3 : (x_1^*, x_2^*) = \left(\frac{\mu + 1 + \sqrt{(\mu+1)(\mu-3)}}{2\mu}, \frac{\mu + 1 - \sqrt{(\mu+1)(\mu-3)}}{2\mu} \right), \tag{3}$$

and its $(x_1, x_2) \mapsto (x_2, x_1)$ reflection E_4, exist for $\mu \geqslant 3$.

The study of the local stability of fixed points is based on the linearization of (1). In an equilibrium point the Jacobian $J(x_1, x_2)$ of (1) has the eigenvalues:

$$\lambda_{1,2} = (1 - \mu) \pm \rho\mu\sqrt{(1 - 2x_1)(1 - 2x_2)}. \tag{4}$$

Depending on the values of x_1 and x_2, these may be real or form a conjugate complex pair. A fixed point of (1) is stable if

$$|\lambda_j| < 1, \quad j = 1, 2. \tag{5}$$

Proposition 2.1. *The equilibrium solution E_1 is asymptotically stable for $(\mu, \rho) \in \Omega^{\mathrm{S}}(E_1)$ where*

$$\Omega^{\mathrm{S}}(E_1) = \left\{ (\mu, \rho) | 0 < \mu < 1, 0 < \rho < \rho_1(\mu) = \frac{2}{1+\mu} \right\}.$$

It loses stability via a flip bifurcation when crossing the threshold $\rho_1(\mu)$, $0 < \mu < 1$ and via branching along $\mu = 1$.

Proof. The stability boundaries of E_1 can be derived by imposing the stability conditions (5). These boundaries were computed in [2] and are presented in Fig. 1 ($\Omega^{\mathrm{S}}(E_1)$).

What remains to be proved is that E_1 loses its stability and bifurcates to a new branch of fixed points at $\mu = 1$. To do this we show that the discriminant of the *algebraic branching equation* (ABE), see [16], is positive. We consider the Jacobian matrix $F_X = [T_x - I | T_\mu]$, evaluated in E_1 that is

$$\begin{pmatrix} -\rho & \rho\mu & 0 \\ \rho\mu & -\rho & 0 \end{pmatrix}. \tag{6}$$

This matrix is clearly rank deficient along $\mu = 1$. We first compute vectors ϕ_1, ϕ_2 and ψ which form a basis for the null space of $N([T_x - I|T_\mu])$ and $N([T_x - I|T_\mu]^*)$, respectively. Possible choices are

$$\phi_1 = \left(\frac{1}{\sqrt{2}}, \frac{1}{\sqrt{2}}, 0\right)^{\mathrm{T}}, \quad \phi_2 = (0, 0, 1)^{\mathrm{T}}, \quad \psi = \left(\frac{1}{\sqrt{2}}, \frac{1}{\sqrt{2}}\right)^{\mathrm{T}}.$$

Now we consider the ABE:

$$c_{11}\alpha^2 + 2c_{12}\alpha\beta + c_{22}\beta^2 = 0, \tag{7}$$

where $c_{jk} = \langle \psi, F^0_{YY}\phi_j\phi_k\rangle$, for $j, k = 1, 2$. Here the $2 \times 3 \times 3$ tensor F^0_{YY} is given by

$$F^0_{YY}(:, :, 1) = \begin{pmatrix} 0 & 0 & 0 \\ -2\mu\rho & 0 & \rho(1 - x_1) - \rho x_1 \end{pmatrix}, \tag{8}$$

$$F^0_{YY}(:, :, 2) = \begin{pmatrix} 0 & -2\mu\rho & \rho(1 - x_2) - \rho x_2 \\ 0 & 0 & 0 \end{pmatrix}, \tag{9}$$

$$F^0_{YY}(:, :, 3) = \begin{pmatrix} 0 & \rho(1 - x_2) - \rho x_2 & 0 \\ \rho(1 - x_1) - \rho x_1 & 0 & 0 \end{pmatrix}. \tag{10}$$

We now obtain $c_{11} = -\sqrt{2}\rho$, $c_{12} = \rho$, $c_{22} = 0$. So the discriminant of (7), $c_{12}^2 - c_{11}c_{22} = \rho^2 > 0$ is clearly positive. This shows that we have a branch point when $\mu = 1$. □

Proposition 2.2. *E_2 is asymptotically stable for $(\mu, \rho) \in \Omega^{\mathrm{S}}(E_2) = \Omega^{\mathrm{S}}(E_{21}) \cup \Omega^{\mathrm{S}}(E_{22})$ where*

$$\Omega^{\mathrm{S}}(E_{21}) = \left\{(\mu, \rho)|1 < \mu < 2, 0 < \rho < \rho_{21}(\mu) = \frac{2}{3 - \mu}\right\},$$

and

$$\Omega^{\mathrm{S}}(E_{22}) = \left\{(\mu, \rho)|2 < \mu < 3, 0 < \rho < \rho_{22}(\mu) = \frac{2}{\mu - 1}\right\}.$$

It loses stability via a flip bifurcation point on the boundaries of

(i) $\rho = \rho_{21}(\mu)$, $1 < \mu < 2$.
(ii) $\rho = \rho_{22}(\mu)$, $2 < \mu < 3$.

Furthermore, it loses stability via a branch point when $\mu = 1$ and 3.

Proof. The stability domain of E_2 is given in [2] and presented in Fig. 1 ($\Omega^{\mathrm{S}}(E_2)$). By the same procedure as in Proposition 2.1, we can show that E_2 bifurcates to the branches of fixed points E_1 and $E_3(E_4)$ at $\mu = 1$ and 3, respectively. □

Proposition 2.3. *E_3 (E_4) is asymptotically stable for $(\mu, \rho) \in \Omega^{\mathrm{S}}(E_3) = \Omega^{\mathrm{S}}(E_{31}) \cup \Omega^{\mathrm{S}}(E_{32})$ where*

$$\Omega^{\mathrm{S}}(E_{31}) = \left\{(\mu, \rho)|3 < \mu < 1 + \sqrt{5}, 0 < \rho < \rho_{31}(\mu) = \frac{2}{1 + \sqrt{5 - (\mu - 1)^2}}\right\},$$

and

$$\Omega^{\mathrm{S}}(E_{32}) = \left\{(\mu, \rho)|\mu > 1 + \sqrt{5}, 0 < \rho < \rho_{32}(\mu) = \frac{2}{(\mu - 1)^2 - 4}\right\}.$$

It loses stability:

(i) *via a flip point when* $\rho = \rho_{31}(\mu)$, $3 < \mu < 1 + \sqrt{5}$.
(ii) *via a Neimark–Sacker bifurcation point when* $\rho = \rho_{32}(\mu)$, $\mu > 1 + \sqrt{5}$.

Moreover, it loses stability and bifurcates to the branch of E_2 *fixed points along* $\mu = 3$.

Proof. The stability boundaries of E_3 were computed in [2] and are sketched in Fig. 1 ($\Omega^S(E_{3,4})$). It is easy to prove that E_3 bifurcates to a branch of fixed points E_2 at $\mu = 3$, by the same procedure as in Proposition 2.1. □

Proposition 2.4. *The flip bifurcation in Proposition* 2.1 *is subcritical*.

Proof. We show that E_1 undergoes a subcritical flip when $\rho = 2/(1+\mu)$, $0 < \mu < 1$. It is sufficient to show that the critical normal form coefficient b,

$$b = \frac{1}{6}\langle p, C(q,q,q) + 3B(q,(I - A^{(1)})^{-1}B(q,q))\rangle, \tag{11}$$

derived by the parameter-dependent center manifold reduction is negative, see [18, Chapter 8 and 16], where $A^{(1)}$ is the Jacobian of (1) at E_1, $B(.,.)$ and $C(.,.,.)$ are the second and third order multilinear forms, respectively, p and q are the left and right eigenvectors of $A^{(1)}$, respectively. These vectors are normalized by $\langle p, q\rangle = 1$, $\langle q, q\rangle = 1$, where $\langle .,. \rangle$ is the standard scalar product in R^2. We obtain

$$q = \begin{pmatrix} q_1 \\ q_2 \end{pmatrix} = p = \begin{pmatrix} p_1 \\ p_2 \end{pmatrix} = \begin{pmatrix} \frac{1}{\sqrt{2}} \\ -\frac{1}{\sqrt{2}} \end{pmatrix}, \tag{12}$$

$$[B(q,q)]_1 = \sum_{j,k=1}^{n} \frac{\partial^2((1-\rho)x_1 + \rho\mu x_2(1-x_2))}{\partial x_j \partial x_k} q_j q_k = -2\rho\mu q_2 q_2 = -\rho\mu, \tag{13}$$

$$[B(q,q)]_2 = \sum_{j,k=1}^{n} \frac{\partial^2((1-\rho)x_2 + \rho\mu x_1(1-x_1))}{\partial x_j \partial x_k} q_j q_k = -2\rho\mu q_1 q_1 = -\rho\mu. \tag{14}$$

Let $\zeta = (I - A^{(1)})^{-1}B(q,q)$, then we have $\zeta = \begin{pmatrix} \frac{\mu}{\mu-1} \\ \frac{\mu}{\mu-1} \end{pmatrix}$ and find

$$[B(q,\zeta)]_1 = -\rho\mu q_2\zeta_2 = \sqrt{2}\frac{\rho\mu^2}{\mu-1}, \quad [B(q,\zeta)]_2 - \rho\mu q_1\zeta_1 = -\sqrt{2}\frac{\rho\mu^2}{\mu-1}. \tag{15}$$

Since the third order multilinear form $C(q,q,q)$ is zero, the critical normal form coefficient b is given by $b=\rho\mu^2/(\mu-1)$. It is clear that $b < 0$, since $0 < \mu < 1$ and $\rho > 0$ in $\Omega^S(E_1)$. □

Proposition 2.5. *The flip point in Proposition* 2.2 *is sub- or supercritical in cases* (i) *and* (ii), *respectively*.

Proof. First we consider case (i) and show that the flip point is subcritical. It is sufficient to show that $b < 0$ where b is defined in (11). The normalized left and right eigenvectors for $A^{(2)}$ are given by

$$q = \begin{pmatrix} q_1 \\ q_2 \end{pmatrix} = p = \begin{pmatrix} p_1 \\ p_2 \end{pmatrix} = \begin{pmatrix} \frac{1}{\sqrt{2}} \\ -\frac{1}{\sqrt{2}} \end{pmatrix}, \tag{16}$$

where $A^{(2)}$ is the Jacobian of (1) at E_2. $B(q,q)$ is given by

$$[B(q,q)]_1 = -2\rho\mu q_2 q_2 = -\rho\mu, \quad [B(q,q)]_2 = -2\rho\mu q_1 q_1 = -\rho\mu. \tag{17}$$

We proceed with the computation of $\zeta = (I - A^{(2)})^{-1} B(q, q)$ and obtain

$$\zeta = \begin{pmatrix} \frac{\mu}{1-\mu} \\ \frac{\mu}{1-\mu} \end{pmatrix}, \quad b = \frac{\rho\mu^2}{1-\mu}. \tag{18}$$

So $b < 0$, since $1 < \mu < 2$ and $\rho > 0$ in $\Omega^S(E_2)$.

In case (ii) we obtain $b = \rho\mu^2/3(\mu - 1)$. So $b > 0$, since $2 < \mu < 3$ and $\rho > 0$ in $\Omega^S(E_2)$. □

Proposition 2.6. *The flip bifurcation in Proposition* 2.3 *is subcritical*.

Proof. Similar to the previous cases we show that the critical normal form coefficient $b < 0$. The Jacobian matrix (1) at E_3 (E_4) is

$$A^{(3)} = \begin{pmatrix} 1 - \rho & -\rho(1 + \sqrt{(\mu + 1)(\mu - 3)}) \\ -\rho(1 - \sqrt{(\mu + 1)(\mu - 3)}) & 1 - \rho \end{pmatrix}, \tag{19}$$

and has a multiplier -1 when $\rho = 2/(1 + \sqrt{5 - (\mu - 1)^2})$, $3 < \mu < 1 + \sqrt{5}$. The left and right eigenvectors associated to the eigenvalue -1 are given by

$$q = \begin{pmatrix} -\sqrt{4 - \mu^2 + 2\mu} \\ -1 + \sqrt{-3 + \mu^2 - 2\mu} \end{pmatrix}, \quad p = \begin{pmatrix} -1 + \sqrt{-3 + \mu^2 - 2\mu} \\ -\sqrt{4 - \mu^2 + 2\mu} \end{pmatrix}. \tag{20}$$

To avoid complicated computations we do not normalize p and q, since rescaling does not change the sign of b provided $\langle p, q \rangle > 0$ (it can be proved easily that this is the case). $B(q, q)$ is computed as:

$$B(q, q) = \begin{pmatrix} \dfrac{4\mu(-1 + \sqrt{(-3 + \mu^2 - 2\mu)^2})}{(1 + \sqrt{4 - \mu^2 + 2\mu})(-4 + \mu^2 - 2\mu)} \\ -\dfrac{4\mu}{(1 + \sqrt{4 - \mu^2 + 2\mu})} \end{pmatrix}. \tag{21}$$

The vector $\zeta = (I - A^{(3)})^{-1} B(q, q)$, is given by

$$\zeta = \begin{pmatrix} \dfrac{2\mu(-1 + \sqrt{(-3 + \mu^2 - 2\mu)^2}}{(\mu + 1)(\mu - 3)(-4 + \mu^2 - 2\mu)} + \dfrac{2(1 + \sqrt{(\mu + 1)(\mu - 3)})}{(\mu + 1)(\mu - 3)} \\ \dfrac{2(-1 + \sqrt{(\mu + 1)(\mu - 3)})\mu(-1 + \sqrt{(-3 + \mu^2 - 2\mu)^2})}{(\mu + 1)(\mu - 3)(-4 + \mu^2 - 2\mu)} - \dfrac{2\mu}{(\mu + 1)(\mu - 3)} \end{pmatrix}. \tag{22}$$

$B(q, \zeta)$ can be computed from (20) and (22):

$$B(q, \zeta) = \begin{pmatrix} -\dfrac{8(12-4\mu^2+8\mu+\sqrt{(-3+\mu^2-2\mu)}\mu^2-2\sqrt{(-3+\mu^2-2\mu)}\mu)(-1+\sqrt{(-3+\mu^2-2\mu)})\mu^2}{(4-\mu^2+2\mu)^{\frac{3}{2}}(\mu-3)(\mu+1)(1+\sqrt{(4-\mu^2+2\mu)})} \\ -\dfrac{8(-6-6\sqrt{(-3+\mu^2-2\mu)}+2\mu^2-4\mu + \sqrt{(-3 + \mu^2 - 2\mu)}\mu^2 - 2\sqrt{(-3 + \mu^2 - 2\mu)}\mu)\mu^2}{(-4 + \mu^2 - 2\mu)(\mu - 3)(\mu + 1)(1 + \sqrt{4 - \mu^2 + 2\mu})} \end{pmatrix}. \tag{23}$$

Finally, the normal form coefficient b can be computed:

$$b = -\frac{576(\mu^2 - 2\mu - 2\sqrt{-3 + \mu^2 - 2\mu} - 2)\mu^2}{(1 + \sqrt{4 - \mu^2 + 2\mu})(-4 + \mu^2 - 2\mu)^2}. \tag{24}$$

We will prove that the factor $h_1(\mu) = \mu^2 - 2\mu - 2(\sqrt{-3 + \mu^2 - 2\mu} + 1)$ in (24) is positive when $3 < \mu < 1 + \sqrt{5}$. Equivalently we have to prove that $(\mu^2 - 2\mu - 2)^2 - 4(\mu^2 - 2\mu - 3) \geqslant 0$. Since $\mathrm{d}h_1/\mathrm{d}\mu(\mu) = 4(\mu - 1)(\mu^2 - 2\mu - 4) < 0$, $h_1(3) = 1$ and $h_1(1 + \sqrt{5}) = 0$, we conclude $h_1 \geqslant 0$. So $b < 0$. □

We remark that our numerical evidence indicates that the Neimark–Sacker bifurcation in Proposition 2.3 is supercritical. This is based on the numerical computation of the normal form coefficient d (see [18, Chapter 8 , 16]). However, we were not able to prove this analytically.

3. Numerical bifurcation analysis in the economically relevant region

In this section we concentrate on the region $\rho \leqslant 1$ which is economically relevant. Since a complete analytical bifurcation study of the iterates of (1) is not feasible, we perform a numerical bifurcation analysis by using the MATLAB package Cl_MatContM, see [14,16]. The bifurcation analysis is based on continuation methods, tracing out the solution manifolds of fixed points while some of the parameters of the map vary, see [7].

3.1. Numerical bifurcation of E_2

By continuation of E_2 with $\mu = 2.5$ and ρ free, we see that E_2 loses stability via a supercritical *PD* point when crossing the hyperbola $\rho = \rho_{22}(\mu)$. A stable 2-cycle is given by $C_2 = \{X_1^2, X_2^2\}$ where $X_1^2 = (0.658212, 0.658212)$, $X_2^2 = (0.527341, 0.527341)$, for $\rho = 1.366229$. This 2-cycle loses stability at a supercritical *PD* point (of the second iterate) for $\rho = 1.490763$. A stable 4-cycle is given by $C_4 = \{X_1^4, X_2^4, X_3^4, X_4^4\}$ where $X_1^4 = (0.3851221, 0.479532)$, $X_2^4 = (0.745563, 0.649279)$, $X_3^4 = (0.479532, 0.38512201)$, $X_4^4 = (0.649279, 0.745563)$.

The multipliers of the fixed point of the fourth iterate in X_1^4 are 0.406438 and 0.129274. This 4-cycle with the parameter values is depicted in Fig. 2. We note that the 4-cycle is invariant under the reflection $(x_1, x_2) \mapsto (x_2, x_1)$.

This 4-cycle loses stability via a supercritical Neimark–Sacker bifurcation.

Stability regions of the 2-cycles ($\Omega_2^{S,i}$, $i = 1, 2, 3$) and 4-cycles ($\Omega_4^{S,i}$, $i = 1, 2, 3$) are given in Fig. 3. They stretch into the economically relevant region $\rho \leqslant 1$. In this figure the regions $\Omega_2^{S,2}$ and $\Omega_4^{S,2}$ indicate bistability of 2- and 4-cycles with E_3 (E_4), respectively. We note that the stability region of the 2-cycle is bounded by the PD^2 curve and a curve of branch points of the second iterate, when $\mu \geqslant 3$. This curve of branch points bifurcates from the *LPPD* point on the *PD*

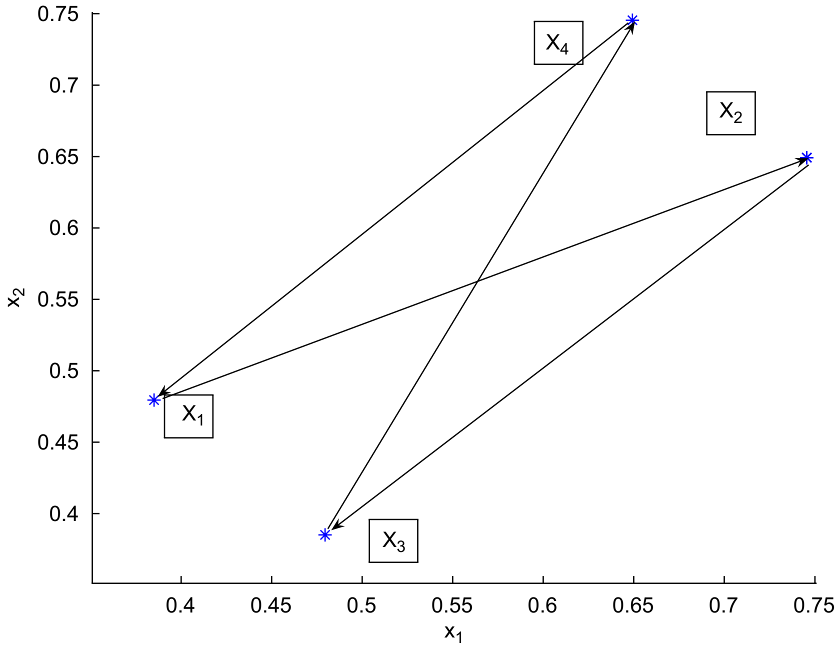

Fig. 2. A stable 4-cycle for $\rho = 1.509191$ and $\mu = 2.5$.

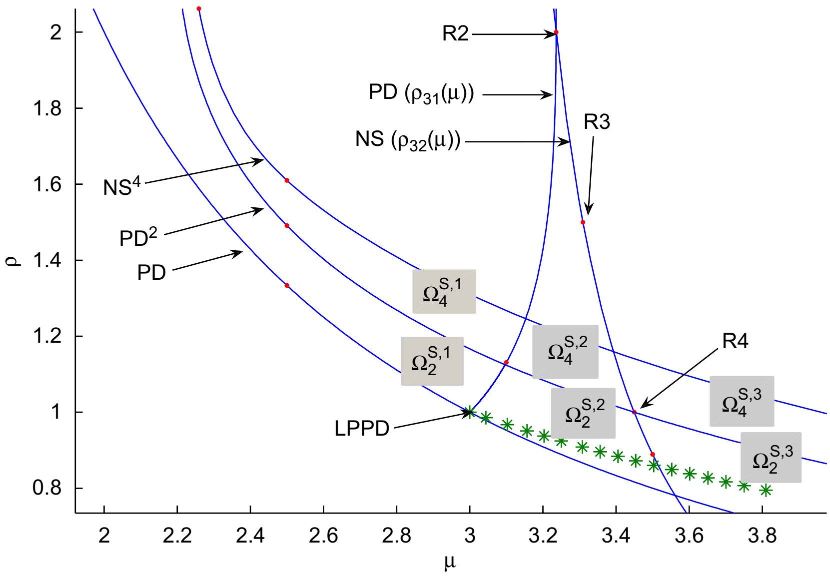

Fig. 3. The Neimark–Sacker curve of *Run* 2, the flip curve of *Run* 6 of Section 4 and the curve of branch points of the second iterate, the stability regions of Ω_2^S and Ω_4^S in (μ, ρ) space.

curve of the original map. This curve is shown by $*$ in Fig. 3 and is completely in the economically relevant region. We note that the *LPPD* point is on the boundary of the economically relevant region.

3.2. Numerical bifurcation study of E_3 (E_4)

We now do a continuation of the fixed point E_3 starting from $\mu = 4,\ \ \rho = 0.1$ in the stable region bounded by the curve $\rho = \rho_{32}(\mu)$. The parameter ρ is free, we call this *Run* 1:

```
label=NSm, x=(0.904508 0.345492 0.400000)
normal form coefficient of NSm =-7.372800e+000
```

A supercritical Neimark–Sacker bifurcation point is detected for $\rho = 0.4$. Thus, the fixed point E_3 (E_4) is transformed from stable to unstable through an *NS* point at which a closed invariant curve is created around the unstable fixed point E_3 (E_4). We now compute the Neimark–Sacker curve, by starting from the *NS* point in *Run* 1, with free parameters μ and ρ, this is *Run* 2:

```
label =R4 , x =( 0.849938 0.439960 1.000000 3.449490 0.0000 )
normal form coefficient of R4 : A =-3.000000e+000 + -2.019371e-017i
label =R3 , x =( 0.825542 0.476627 1.500000 3.309401 -0.500)
normal form coefficient of R3 : Re(c_1) =-1.333333e+000
label =R2 , x =( 0.809017 0.500000 2.000000 3.236068 -1.00 )
normal form coefficient of R2 : [c , d] =1.340433e+003, -3.351046e+003
```

A picture of the Neimark–Sacker curve of *Run* 2 is given in Fig. 3.

Since the $R2$ and $R3$ points are not in the region $\rho \leqslant 1$ we postpone their study to Section 4.

We now consider the $R4$ point in *Run* 2. Since $|A| > 1$, two cycles of period 4 of the map are born. A stable 4-cycle for $\rho = 0.990844$ and $\mu = 3.466353$ is given by $C_4 = \{X_1, X_2, X_3, X_4\}$ where $X_1 = (0.841774, 0.407047)$, $X_2 = (0.836685, 0.461186)$, $X_3 = (0.861140, 0.473539)$, $X_4 = (0.864133, 0.4150395)$. We present this cycle in Fig. 4. We note that it is not invariant under the reflection $(x_1, x_2) \mapsto (x_2, x_1)$. The multipliers in X_1 are $\lambda_1 = 0.901140$ and $\lambda_2 = 0.675526$, confirming the stability of the 4-cycle.

To determine the stability domain of the 4-cycle we compute in *Run* 3 two branches of fold curves of the fourth iterate, emanating from the $R4$ point, by switching at the $R4$ point. These fold curves exist because $|A| > 1$, where A

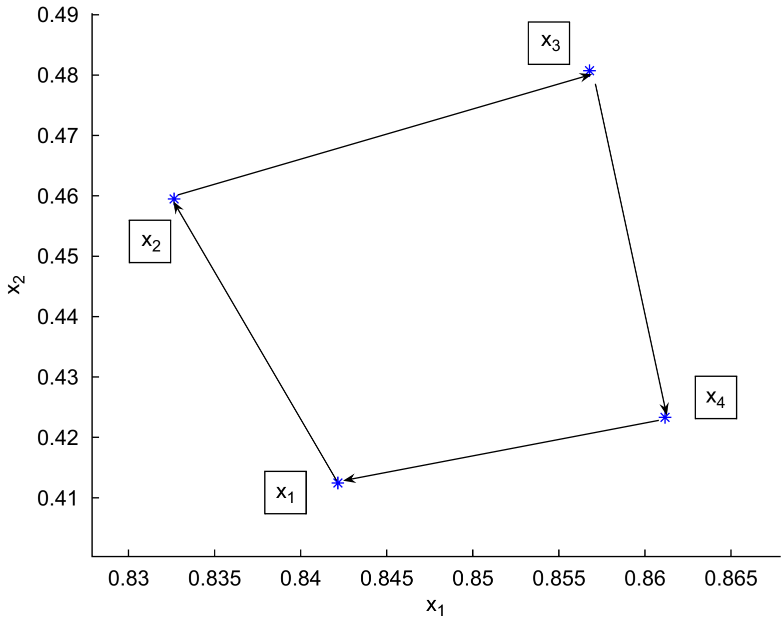

Fig. 4. A stable 4-cycle for $\rho = 0.9999617$ and $\mu = 3.449802$.

is the normal form coefficient of the $R4$ point. The stable fixed points of the fourth iterate exist in the wedge between the two fold curves. We note that there is no bistability with fixed points of the original map.

```
label =CP, x =(0.849982 0.439945 0.999745 3.449889)
normal form coefficient of CP s=4.009280e+002
label =LPPD , x =(0.841586 0.354516 0.935299 3.566686)
normal form coefficient of LPPD :[a/e , be]=
2.574002e+000, -5.829597e+001
label =CP, x =( 0.849982 0.439945 0.999745 3.449889 )
normal form coefficient of CP s=4.009280e+002
label =LPPD , x =( 0.836428 0.522216 1.071080 3.486079 )
normal form coefficient of LPPD :[a/e , be]=
1.733856e+000, -2.471512e+001
```

Two cusps, *CP*, and two *LPPD* bifurcation points are detected on the fold branches of the fourth iterate. The *CP* points are merely the $R4$ point from which we started. We can further compute the stability boundaries of the 4-cycle by computing the flip curve of the fourth iterate rooted at the detected *LPPD* points. The stable region Ω_4^S of C_4 is bounded by two fold curves and a flip curve of the fourth iterate, see Fig. 5. Furthermore, if we continue the fixed point of the fourth iterate starting from X_1, it loses stability via a supercritical *PD* point where $\mu = 3.545530$. It means that a stable 8-cycle is born when $\mu > 3.545530$.

We note that we have bistability of three different 4-cycles in a region bounded by the curves of the *PD* of the second iterate, a fold and the *PD* curve of the fourth iterate. This region is shown as $\Omega_{4,4}^S$ in Fig. 6. Furthermore, we have a small bistability region of two 4-cycles and a 2-cycle. This bistability region is shown as $\Omega_{2,4}^S$ in Fig. 6.

4. Bifurcations of E_3 (E_4) in the region $\rho > 1$

Now we consider the $R2$ point computed in *Run* 3 of Section 3.2. Since the first component of the normal form coefficient $c = 1.340433e + 003$ is positive, the bifurcation scenario near the $R2$ point is analogous to [18, Fig. 9] (case $s = 1$). For the parameter values in the wedge between the *PD* (ρ_{31}) and *NS* (ρ_{32}) curves, the map has an unstable 2-cycle that coexists with a stable fixed point.

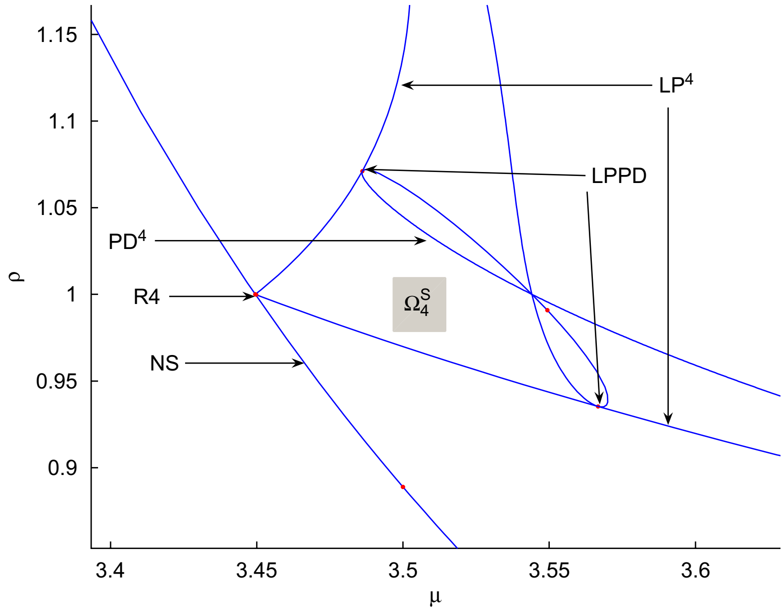

Fig. 5. Two fold bifurcation curves of the fourth iterate emanate from the $R4$ point in (μ, ρ) space.

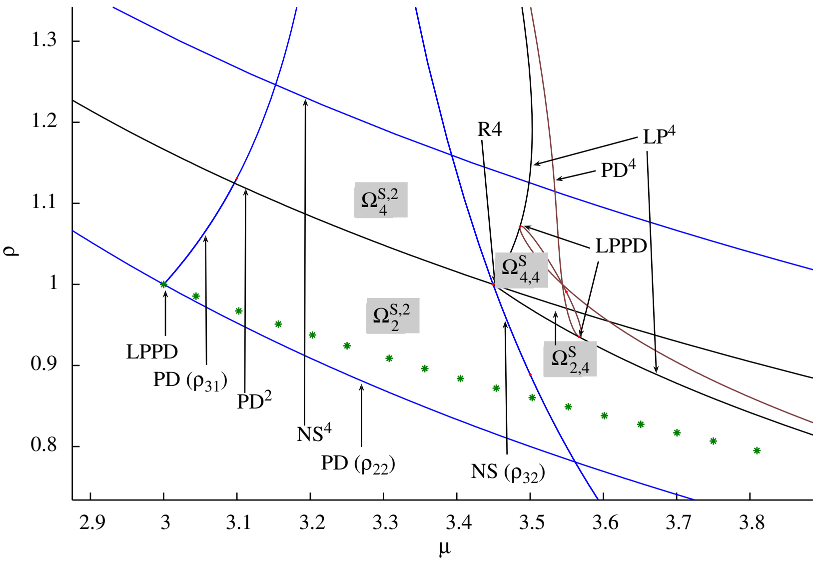

Fig. 6. Bistability regions of 4-cycles, 2-cycles and fixed points.

Next we consider the resonance 1:3 point in *Run* 3 of Section 3.2. Since its normal form coefficient is negative, the bifurcation picture near the $R3$ point is qualitatively the same as presented in [18, Fig. 9]. In particular, there is a region near the $R3$ point where a stable invariant closed curve coexists with an unstable fixed point. For parameter values close to the $R3$ point, the map has a saddle cycle of period three.

Furthermore, a Neutral Saddle bifurcation curve of fixed points of the third iterate emanates. We compute this curve by branch switching at the $R3$ point of *Run* 5. This curve is presented in Fig. 7. Further, a stable 3-cycle exists not far from the $R3$ point (this is not guaranteed by the theory but it is found in many examples, e.g [15]). The stability region of this cycle is bounded by *fold* and *NS* bifurcation curves of the third iterate of the map (Ω_3^S). These boundary curves

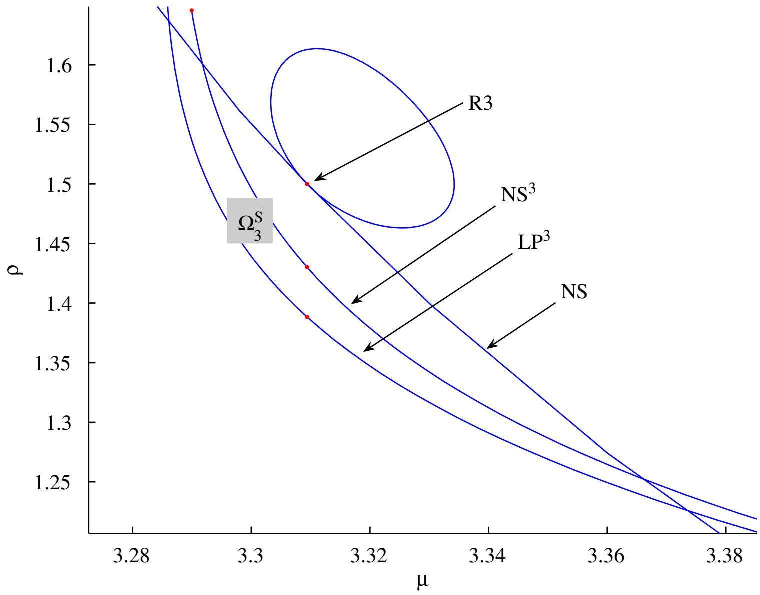

Fig. 7. Two stability boundary curves (*LP* and *NS*) for the stable 3-cycle, together with the *NS* curve of *Run* 3 and the curve of Neutral Saddle bifurcation points of the third iterate.

are given in Fig. 7. We have bistability of the fixed point E_3 (E_4) with the fixed point of the third iterate of the map in the region that is bounded by the fold and *NS* curves and the hyperbola $\rho = \rho_{32}(\mu)$.

5. Conclusions

We studied the dynamical behavior of the Kopel model and computed the stability boundaries of 2-, 3- and 4-cycles. We showed analytically that the trivial fixed point E_1 undergoes a subcritical flip bifurcation when $\rho = \rho_1(\mu)$. The nontrivial symmetric fixed point E_2 loses its stability via a subcritical flip point when crossing the curve $\rho = \rho_{21}(\mu)$, whereas it loses stability along the curve $\rho = \rho_{22}(\mu)$ via a supercritical flip point.

For E_3 (E_4) the transition of stability to unstability is possible via a subcritical flip point when crossing the curve $\rho = \rho_{31}(\mu)$ and via a supercritical Neimark–Sacker point when crossing the curve $\rho = \rho_{32}(\mu)$. E_1 branches to E_2 along $\mu = 1$ and E_2 branches to E_3 (E_4) when $\mu = 3$.

In the case of E_2, the stability domain of the 2-cycle is bounded by two flip curves of the first and second iterates when $1 \leqslant \mu < 3$ and by flip and branch point curves of the second iterate when $\mu \geqslant 3$. These stability domains are shown as $\Omega_2^{S,i}$, $i = 1, 2, 3$ in Fig. 3. We have bistability of E_3 (E_4) and a 2-cycle in $\Omega_2^{S,2}$. The stability domain of the 4-cycle is bounded by curves of flip and Neimark–Sacker bifurcations of the second and fourth iterates, respectively. These stability domains are shown as $\Omega_4^{S,i}$, $i = 1, 2, 3$ in Fig. 3. Moreover, we have bistability of E_3 (E_4) and a 4-cycle in $\Omega_4^{S,2}$.

In the case of E_3 (E_4), the stability domain of the 4-cycle is bounded by two branches of fold curves and a flip curve of the fourth iterate, and shown as Ω_4^S in Fig. 5.

The stability domain of the 3-cycle is bounded by curves of fold and Neimark–Sacker bifurcations of the third iterate; we have bistability of the fixed point of the map and the 3-cycle.

We have bistability of three different 4-cycles in $\Omega_{4,4}^S$ in Fig. 6 and bistability of two 4-cycles and a 2-cycle in $\Omega_{2,4}^S$ in Fig. 6.

We note that for $\rho \in [0, 1]$, the stability regions of cycles are economically interesting. This applies to the stability of 2- and 4-cycles in Fig. 3, stability of the 4-cycle in Fig. 5, bistability of two 4-cycles as well as bistability of 2- and 4-cycles in Fig. 6.

Acknowledgment

The authors thank the referee for several suggestions which have substantially improved the paper, in particular with respect to the economic background of the paper and the relevance of the obtained results.

References

[1] H.N. Agiza, Explicit stability zones for Cournot games with 3 and 4 competitors, Chaos Solitons Fractals 9 (1998) 1955–1966.
[2] H.N. Agiza, On the analysis of stability, bifurcation, chaos and chaos control of Kopel map, Chaos Solitons Fractals 10 (1999) 1909–1916.
[3] H.N. Agiza, G.I. Bischi, M. Kopel, Multistability in a dynamic Cournot game with three oligopolists, Math. Comput. Simulation 51 (1999) 63–90.
[4] H.N. Agiza, A.A. Elsadany, M. Kopel, Nonlinear dynamics in the Cournot duopoly game with heterogeneous players, Physica A 320 (2003) 512–524.
[5] H.N. Agiza, A.S. Hegazi, A.A. Elsadany, Complex dynamics and synchronization of a duopoly game with bounded rationality, Math. Comput. Simulation 58 (2002) 133–146.
[6] E. Ahmed, H.N. Agiza, Dynamics of a Cournot game with n-competitors, Chaos Solitons Fractals 9 (1998) 1513–1517.
[7] E.L. Allgower, K. Georg, Numerical Continuation Methods: An Introduction, Springer, Berlin, 1990.
[8] D.R. Anderson, N.G. Myran, D.L. White, Basin of attraction in a Cournot duopoly model of Kopel, J. Differential Equations Appl. 11 (10) (2005) 879–887.
[9] G.I. Bischi, A. Mammana, L. Gardini, Multistability and cyclic attractors in duopoly games, Chaos Solitons Fractals 11 (2000) 543–564.
[10] J.P. Carcassès, Determination of different configurations of fold and flip bifurcation curves of one or two-dimensional map, Internat. J. Bifur Chaos 3 (4) (1993) 869–902.
[11] J.P. Carcassès, Singularities of the parametric plane of an n-dimensional map, Determination of different configurations of fold and flip bifurcation curves, Int. J. Bifurcation Chaos 5 (2) (1995) 419–447.
[12] J.P. Carcassès, C. Mira, C. Simó, M. Bosch, J.C. Tatjer, "Cross-road area–spring area" transition (I) Parameter plane representation, Internat. J. Bifurcation Chaos 1 (2) (1991) 339–348.
[13] A. Cournot, Researches into the principles of wealth, 1963 (English Translation), Irwin Paperback Classics in Economics (original: Recherches sur les principes mathématiques de la théorie des richesses, 1838).
[14] A. Dhooge, W. Govaerts, Yu.A. Kuznetsov, W. Mestrom, A. Riet, CL_MATCONT: a continuation toolbox in Matlab, 2004, ⟨http://www.matcont.UGent.be⟩.
[15] W. Govaerts, R. Khoshsiar Ghaziani, Numerical bifurcation analysis of a nonlinear stage structured cannibalism population model, J. Differential Equations Appl 12 (10) (2006) 1069–1085.
[16] W. Govaerts, R. Khoshsiar Ghaziani, Yu. A. Kuznetsov, H. Meijer, Bifurcation analysis of periodic orbits of maps in Matlab, 2006, preprint.
[17] M. Kopel, Simple and complex adjustment dynamics in Cournot duopoly models, Chaos Solitons Fractals 12 (1996) 2031–2048.
[18] Yu.A. Kuznetsov, Elements of Applied Bifurcation Theory, third ed., Springer, New York, 2004.
[19] Yu.A. Kuznetsov, H.G.E. Meijer, Numerical normal forms for codim 2 bifurcations of maps with at most two critical eigenvalues, SIAM J. Sci. Comput. 26 (2005) 1932–1954.
[20] C. Mira, J.P. Carcassès, M. Bosch, C. Simó, J.C. Tatjer, "Cross-road area–spring area" transition (II) foliated parametric representation, Internat. J. Bifurcation Chaos 1 (2) (1991) 339–348.
[21] J. Nash, Non-cooperative games, Ann. Math. 54 (1951) 286–295.
[22] T. Puu, Chaos in duopoly pricing, Chaos Solitons Fractals 1 (1991) 573–581.
[23] T. Puu, The Chaotic duopolists revisited, J. Econom. Behav. Organ. 33 (1998) 385–394.
[24] D. Rand, Exotic phenomena in games duopoly models, J. Math. Econom 5 (1978) 173–184.
[25] J.B. Rosser, The development of complex oligopoly dynamics theory, in: T. Puu, I. Sushko (Eds.), Text Book Oligopoly Dynamics: Models and Tools, Springer, Berlin, 2002, pp. 31–83.